

# PROCESSING OF ZIRCONIA AND CALCIUM ALUMINATE CEMENT MIXTURES BY SPARK PLASMA SINTERING

#Y. L. BRUNI\*, G. SUAREZ\*, Y. SAKKA\*\*, L. B. GARRIDO\*, E.F. AGLIETTI\*

\*CETMIC (Centro de Tecnología de Recursos Minerales y Cerámica, CIC-CONICET La Plata)  
Camino Centenario y 506. C.C.49 (B1897ZCA) M.B. Gonnet. Buenos Aires. Argentina

\*\*Fine Particle Processing Group, Nano Ceramics Center, National Institute for Materials Science (NIMS),  
1-2-1, Sengen, Tsukuba, Ibaraki 305-0047, Japan

#E-mail: yesibruni@yahoo.com.ar

Submitted June 8, 2015; accepted September 8, 2015

**Keywords:** Calcia stabilized ZrO<sub>2</sub>, Spark plasma sintering, High alumina cement

*Spark Plasma sintering (SPS) was applied for the densification of Calcia stabilized ZrO<sub>2</sub> based composites obtained from mixtures of pure zirconia (m-ZrO<sub>2</sub>) and calcium aluminate cement (HAC). Two commercial powders of pure zirconia were employed as reactants. One of these powders had a coarse mean particle size ( $d_{50} = 8 \mu\text{m}$ ) and the other was a submicrometer sized powder ( $d_{50} = 0.44 \mu\text{m}$ ). Several compositions containing different proportions of HAC (5 to 30 mol. % CaO in ZrO<sub>2</sub>) were sintered by SPS at temperatures between 1200 and 1400°C under a pressure of 100 MPa during 10 min. The effect of processing conditions on phase composition, densification, microstructure and Vickers hardness of the obtained composites was examined. SPS significantly enhanced the densification in both type of composites (relative density > 93 %) as compared to those previously produced by conventional sintering. Composites with low CaO content consisted of mixtures of c-ZrO<sub>2</sub>, (Ca<sub>0.15</sub>Zr<sub>0.85</sub>O<sub>1.83</sub>), unreacted m-ZrO<sub>2</sub> and calcium dialuminate (CaAl<sub>2</sub>O<sub>7</sub> or CA<sub>2</sub>). The highest hardness was determined for composites sintered at 1400°C being related to the maximum relative density (~ 99 %). High densification of composites with 30 mol. % CaO composed by similar proportions of CaAl<sub>2</sub>O<sub>7</sub> and c-ZrO<sub>2</sub> were obtained even at 1200°C but led to a slightly lower hardness. In general, the use of the finer m-ZrO<sub>2</sub> powder contributed to increase both the c-ZrO<sub>2</sub> content and densification of composite sintered at a relatively lower temperature. For these composites, best hardness (Hv near to 10 GPa) resulted when the microstructure consisted of a fine grained ZrO<sub>2</sub> matrix surrounding the dispersed CaAl<sub>2</sub>O<sub>7</sub> grains instead of large interconnection between grains of both phases existed.*

## INTRODUCTION

Spark Plasma Sintering (SPS) is an effective method for the consolidation and rapid sintering of ceramics to full densification. The combination of high heating rate, and the effects of electric field and pressure enhance the driving force for densification [1]. The high heating rates result in a benefit by passing the grain coarsening low temperature mechanisms (e.g. surface diffusion) and, in many cases, inhibit the grain growth. The influence of electric current on mass transport is attributed to several mechanisms including electromigration and intensified diffusion in ionic conductors, electroplasticity [2] and also to other effects at microstructural level such as the increase in point defect concentration, or a reduction in the mobility activation energy for defects [3]. Pressure applied during SPS affects sintering as a result of particle re-arrangement and the disintegration of soft aggregates, and also provides an intrinsic contribution to the driving force on sintering [1, 4].

The SPS presents many advantages in comparison with several conventional sintering methods including pressureless sintering, hot-pressing and others, such as lower sintering temperature and shorter holding time

that produce comparative improvements in properties of resulting products [1, 5-7]. Pressure and lower sintering temperatures limit grain growth compared to conventional sintering, but coarsening is never totally suppressed [8].

Previous studies reported that SPS was effective for enhancing density and to retain low grain size in alumina and zirconia ceramics [8-15]. In particular previous studies show that SPS improves mechanical properties (flexural strength, Vicker's hardness and fracture toughness) as well as ionic conductivity of 3 and 8 – mol. % Y<sub>2</sub>O<sub>3</sub> stabilized zirconia which, in turn affect their performance as structural ceramics, electrolyte for SOFC, etc. These properties are strongly dependent on the microstructure and processing conditions. Thus, the optimization of sintering parameters such as heating rate, sintering temperature and dwell duration, pressure applied, etc. lead to a successful consolidation of various nano sized ZrO<sub>2</sub> ceramics [8, 14].

CaO is a current stabilizer of commercially available ZrO<sub>2</sub> products and the typical additions vary between 7.5 - 8.7 mol. % in ZrO<sub>2</sub>. Standard partially stabilized ZrO<sub>2</sub> contains approximately 5 mol. % CaO while the full stabilization in the cubic form requires

approximately 20 mol. % [16-19]. Recently, composites with high ZrO<sub>2</sub> content belonging to the ZrO<sub>2</sub>-CaO-Al<sub>2</sub>O<sub>3</sub> system were produced from various mixtures of m-ZrO<sub>2</sub> and high alumina cement (HAC) by conventional (pressureless) sintering [20]. These composites attained a relatively moderate density up to 1500°C indicating the low sinterability of this mixture. The porous composites with open pore structure have potential applications as filters, biomaterials, catalyst, components for SOFC, thermal insulating materials, etc. On the other hand, high densification is beneficial for CaO-ZrO<sub>2</sub> based composites designed for structural, furnace and biomedical applications due to ensure the improvement of the mechanical properties required to the desired application [17-21]. Therefore, the processing by SPS of dense calcia stabilized ZrO<sub>2</sub> based composites obtained from mixtures of m-ZrO<sub>2</sub> and calcium aluminate cement, as a source of calcium, is investigated in this work. The effect of important processing variables such as chemical composition, m-ZrO<sub>2</sub> particle size, sintering temperature (1200 to 1400°C) on the reaction (that leads to the formation of phases corresponding to the ZrO<sub>2</sub>-CaO-Al<sub>2</sub>O<sub>3</sub> system), densification, microstructure and Vicker's hardness were examined. Crystalline phase formation was investigated by X-ray diffraction analysis.

## EXPERIMENTAL

### Starting Materials

Two commercial powders of pure zirconia (monoclinic phase, m-ZrO<sub>2</sub>) were employed as reactants. One of these with coarse particle size (mean particle size  $d_{50} = 8 \mu\text{m}$ ) has a narrow particle size distribution ranging between  $d_{90} = 15 \mu\text{m}$  and  $d_{10} = 5 \mu\text{m}$ ; the other indicated as fine zirconia (mean size  $d_{50} = 0.44 \mu\text{m}$ ) was a submicrometer sized powder (CZE, Saint-Gobain ZirPro) having  $d_{90} = 1.46 \mu\text{m}$  and  $d_{10} = 0.1 \mu\text{m}$ ; with the specific surface area  $5.6 \text{ m}^2 \cdot \text{g}^{-1}$ .

A commercial high alumina cement (HAC) widely used in the refractory industry [22] was the second reactant (Secar 71, Kerneos, France). The main constituents of this cement are Al<sub>2</sub>O<sub>3</sub> and CaO, whose approximate chemical composition (product data sheet) indicates 26.6 - 29.2 wt. % CaO and 69.8 - 72.2 wt. % Al<sub>2</sub>O<sub>3</sub>. The mineralogical composition of HAC was verified using XRD indicating that the major component is calcium monoaluminate (CaAl<sub>2</sub>O<sub>4</sub> or CA) with 25 wt. % of CaAl<sub>4</sub>O<sub>7</sub> or CA<sub>2</sub> and scarce amounts of Al<sub>2</sub>O<sub>3</sub>. A previous study reported that HAC shows specific surface area of  $1.2 \text{ m}^2 \cdot \text{g}^{-1}$  and consists mainly of relatively large particles ranging from 1 to 63  $\mu\text{m}$  with a mean particle size  $d_{50} = 13 \mu\text{m}$  [23]. It should be noted that the HAC has relatively coarser particles when compared to those of the two ZrO<sub>2</sub> powders used.

From these raw materials, two series of powder mixtures were prepared with different chemical com-

positions varying between 5 to 30 mol. % of CaO in ZrO<sub>2</sub>. The composites were identified in this work according to the CaO molar content relative to ZrO<sub>2</sub> and considering the particle size of zirconia powder used as reactant. The composites were named as ZC for the coarse zirconia (mean size  $d_{50} = 8 \mu\text{m}$ ) and ZCF for the fine zirconia (mean size  $d_{50} = 0.44 \mu\text{m}$ ). Thus i.e, ZC5 indicates the ZC composite with 5 mol. % CaO in ZrO<sub>2</sub> and ZCF30 indicates the ZCF composite with 30 mol. % CaO in ZrO<sub>2</sub>.

### SPS system

Densification of the mixed powders was conducted using a SPS machine (SPS-1050, Sumitomo, Japan). The powder was placed into a graphite die with an inner diameter of 10 mm. In a typical sintering experiment, 1.0 g of the mixed powder was poured into the die. The device is composed of an outer and an inner graphite die, with graphite punches; the remaining devices were also made entirely of graphite. The temperature was measured accurately using an optical pyrometer focused on the die surface. Graphite felt was used to reduce the heat loss by radiation. The powder was heated from room temperature up to 700°C within 5 min, subsequently, up to the sintering temperature (1200, 1300, and 1400°C) using a heating rate of  $300^\circ\text{C} \cdot \text{min}^{-1}$ . The dwelling time was 10 min and pressure (100 MPa) was raised just before the holding. Heating was conducted using a sequence consisting of 12 DC pulses (40.8 ms) followed by zero current for 6.8 ms. During the entire duration of the experiments, the electric current intensity was below 1000 A and the voltage drop between the cooled rams was below 4 V.

### Characterization of SPS composites

X-ray diffraction analysis (XRD) was carried out using a Philips diffractometer model PW3020 with radiation Cu-K $\alpha$  and Ni filter in the region  $2\theta$  10 - 80°. The relative proportion of m-ZrO<sub>2</sub> phase was determined quantitatively from the XRD diagrams using the method of Garvie and Nicholson [24] for mixtures of stabilized zirconia and monoclinic phase.

Scanning electron microscopy (SEM, Quanta 200 FEI MK2 Serie) combined with energy dispersive X-ray spectroscopy was used to examine the microstructure development. The obtained results were correlated to composition and SPS temperature.

Apparent density and porosity of the sintered samples was evaluated by Hg immersion. The relative density RD was calculated as a ratio between the apparent and theoretical density of composite which was evaluated considering the volume fraction and the density of each phase present being for m-ZrO<sub>2</sub>, c-ZrO<sub>2</sub> and CaAl<sub>4</sub>O<sub>7</sub> of 5.82, 5.55 and  $2.88 \text{ g} \cdot \text{cm}^{-3}$ , respectively. The volume fraction of each phase was estimated based on XRD

results and the chemical composition. For this, it was considered the relative content of  $c\text{-ZrO}_2$  and the alumina present was as  $\text{CA}_2$  ( $\text{CaAl}_4\text{O}_7$ ).

Hardness (Hv) of the composite was evaluated by Vicker's indentation technique (Buehler durometer, dentamet 1100, Serie Test Macro Vickers) with a load of 1 Kgf during 15 s for each material on polished surfaces up to 1  $\mu\text{m}$ . The hardness reported represents the average value of ten indentations.

## RESULTS AND DISCUSSION

### Crystalline phases present

Figures 1a-c shows the XRD patterns of ZC composites (mixtures with coarse zirconia) sintered at different temperatures (1200, 1300 and 1400°C). The ZC5 and ZC15 composites consisted of a mixture of  $m\text{-ZrO}_2$  and  $c\text{-ZrO}_2$  ( $\text{Ca}_{0.15}\text{Zr}_{0.85}\text{O}_{1.85}$ ) with a small amount of  $\text{CA}_2$  ( $\text{CaAl}_4\text{O}_7$ ) due to the small content of HAC. Therefore the small content of CaO in these composites derived in the lowest formation of  $c\text{-ZrO}_2$  (produced by solid reaction from CaO and  $m\text{-ZrO}_2$ ) at 1200°C and 1300°C being  $m\text{-ZrO}_2$  the main phase. Moreover, the  $c\text{-ZrO}_2$  formation increased with sintering temperature as indicated by the high relative intensity of the characteristic peaks of this phase ( $2\theta$ : 30.15, 34.95, 50.22, 59.68°) and thus was observed that the  $m\text{-ZrO}_2$  phase decreased noticeably at 1400°C.

For ZC30 composites (Figure 1c), the high available amount of HAC resulted in high formation of  $\text{CA}_2$  and  $c\text{-ZrO}_2$ . In fact in these composites the high amount of CaO present and the sintering at 1300 and 1400°C determined a complete transformation of  $m\text{-ZrO}_2$  to  $c\text{-ZrO}_2$  phase.

The  $\text{CA}_2$  was the only crystalline phase formed containing alumina at 1400°C (neither  $\text{CA}_6$  nor  $\alpha\text{-Al}_2\text{O}_3$  were detected by XRD).

It should be noted that the mentioned phases were in agreement to those present in the phase equilibrium diagram of the system ZCA [25]

Figures 2a-c shows the XRD patterns of ZCF composites (mixtures with fine zirconia) sintered at 1200 to 1400°C. These composites presented a similar composition than ZC composites but showed a small increase in  $c\text{-ZrO}_2$  contents with respect to that of the respective ZC composites.

XRD characteristic peaks of each phases appeared slightly broader in both series of composites sintered at 1200°C indicating the presence of small crystallite sizes. Relative narrower peaks in XRD patterns for ZC composites sintered at 1400°C in comparison to those of the ZCF series suggested the high crystallinity of the material.

Figures 3a, b show the variation of relative content of  $c\text{-ZrO}_2$  in percentage (with respect to total  $\text{ZrO}_2$ ) with the CaO content for ZC and ZCF composites sintered at 1200 - 1400°C, respectively.

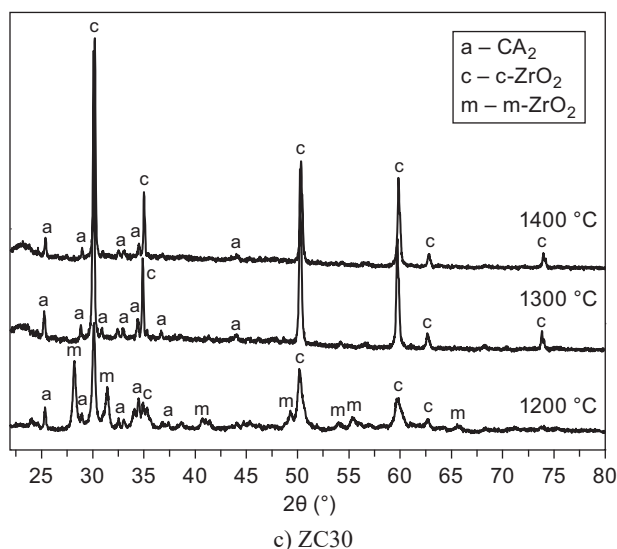
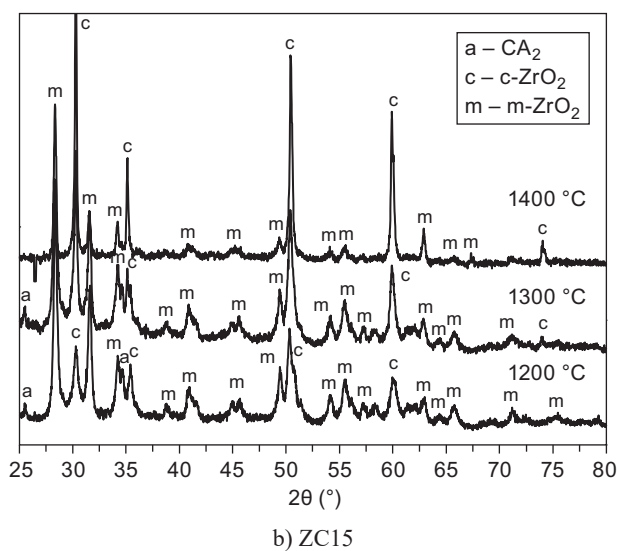
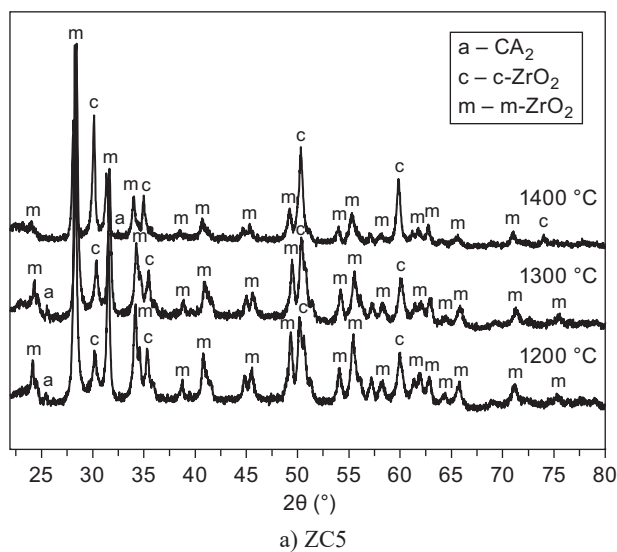
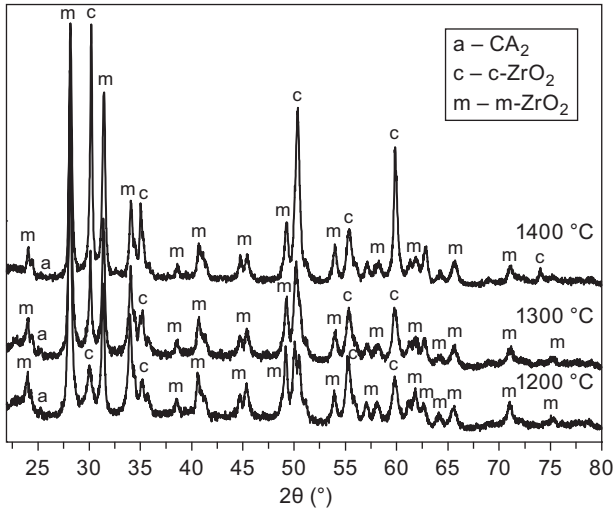
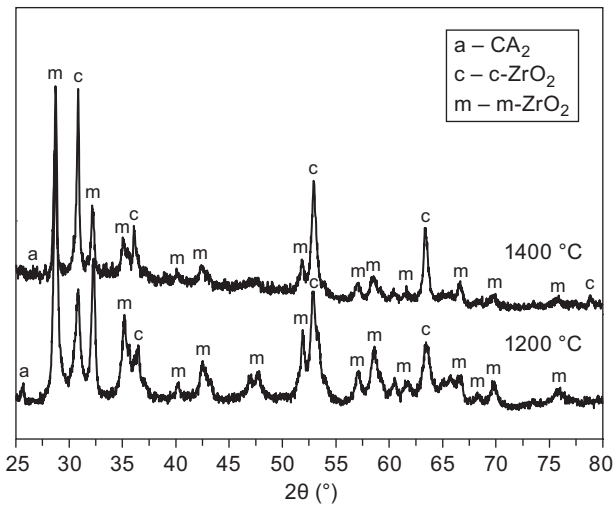


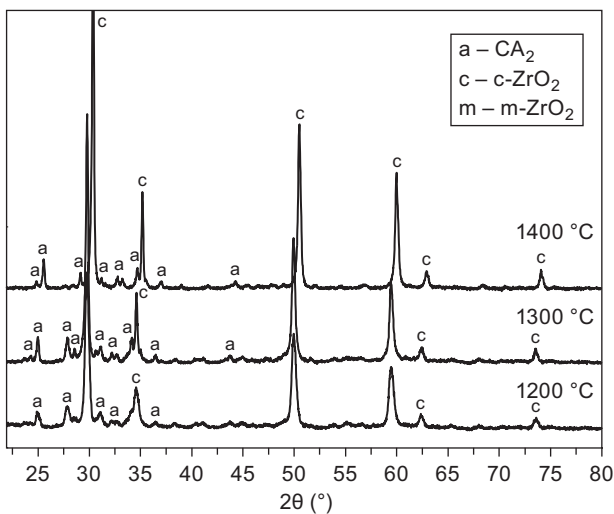
Figure 1. XRD of ZC composites (produced from coarse  $\text{ZrO}_2$ -HAC composition) sintered at 1200-1400°C; a) ZC5, b) ZC15, c) ZC30.



a) ZCF5

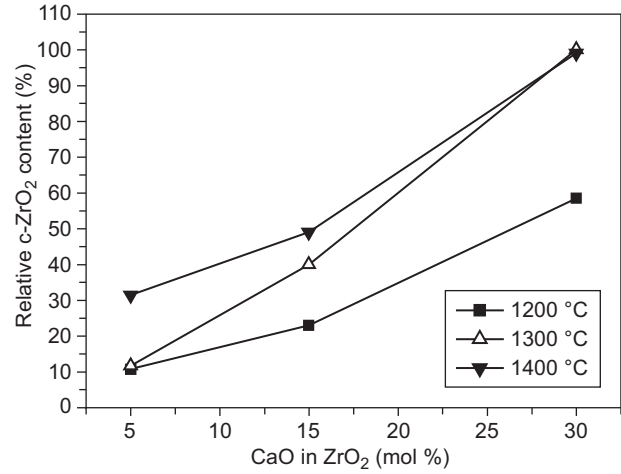


b) ZCF15

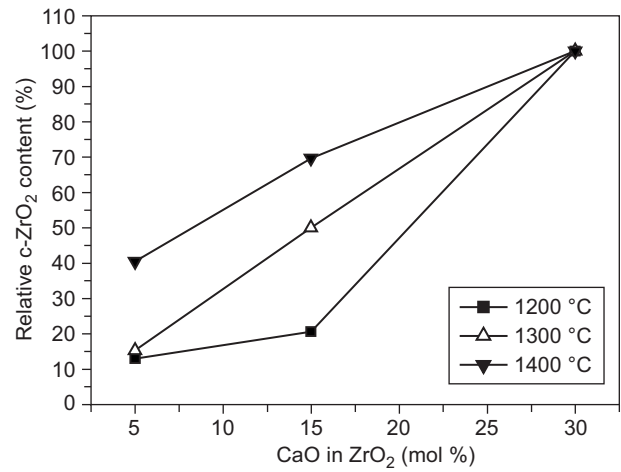


c) ZCF30

Figure 2. XRD of ZCF composites (produced from fine  $ZrO_2$ -HAC composition) sintered at 1200-1400 °C; a) ZCF5, b) ZCF15, c) ZCF30.



a) ZCF



b) ZCF

Figure 3. Evolution of relative c- $ZrO_2$  content with mol. % CaO of composites sintered at different temperatures; a) ZCF composites (coarse  $ZrO_2$ ), b) ZCF composites (fine  $ZrO_2$ ).

In ZCF5 and ZCF15 composites sintered at 1200°C and 1300°C the small content of CaO derived in the lowest formation of c- $ZrO_2$  (less than 20 %). But at 1400°C in these composites was observed an increment of this phase content (30 - 40 % of c- $ZrO_2$ , respectively) that indicated the high effectiveness of the SPS temperature to activate the diffusional processes involved in the reaction (between m- $ZrO_2$  and CaO) for mixtures with low contents of CaO.

In ZCF30 composites the stabilization of zirconia as c- $ZrO_2$  phase was complete at all temperatures (inclusive at 1200°C) due to the high CaO content. In ZCF30 composites the same results was determined at 1300 and 1400°C, while at 1200°C the content of c- $ZrO_2$  only attained 60 %.

The highest stabilization of zirconia as c- $ZrO_2$  phase on ZCF composites inclusive at 1200°C can be explained because the finer  $ZrO_2$  particle size increased contact area between reactant particles enhancing

diffusion of the Ca ion in the lattice of the m-ZrO<sub>2</sub>. The diffusion of Ca ions also seems to be accelerated by the spark plasma sintering, as well as the particle size effect.

In general the formation of c-ZrO<sub>2</sub> phase mainly depends on CaO content. The effect of sintering temperature was significant only at lowest CaO content (i.e. ZC and ZCF composites those containing 5 and 15 mol. % CaO). The effect of low particle size of zirconia (used as starting reactant in ZCF composites) that enhancing c-ZrO<sub>2</sub> formation had a notable influence at the lowest sintering temperature (1200°C) as was previously discussed.

#### Densification

Figures 4a and b show the relative density (RD) of ZC and ZCF composites sintered at 1200, 1300 and 1400°C. This parameter indicated the sintering evolution of these composites with the effect of heat treatment and the CaO content. In general the RD of these composites

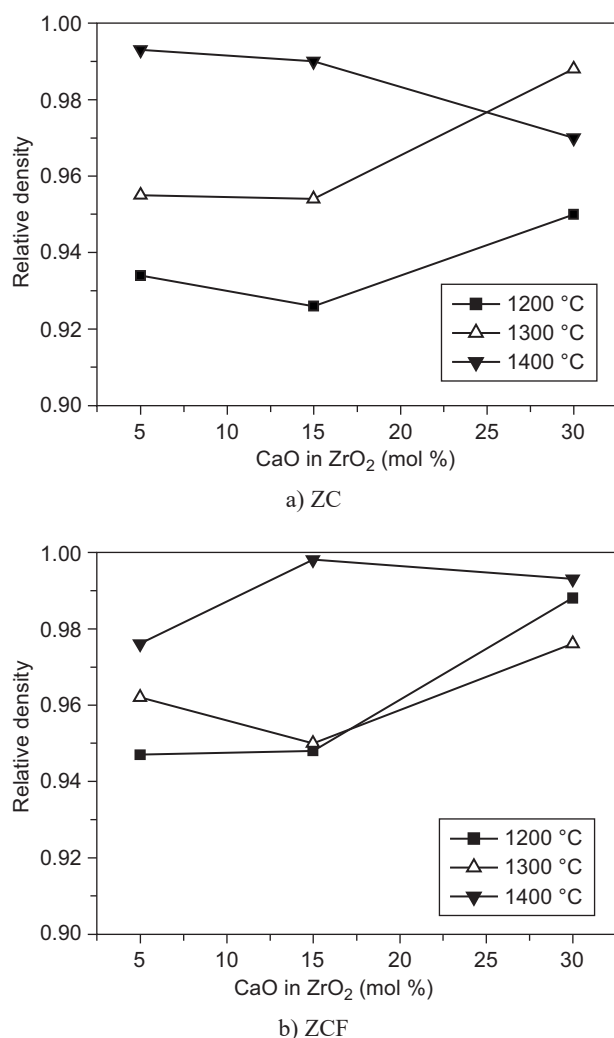


Figure 4. Relative density of composites with 5-30 mol. % CaO sintered at 1200-1400°C; a) ZC composites (coarse ZrO<sub>2</sub>); b) ZCF composites (fine ZrO<sub>2</sub>).

was higher, ranged between 92 % and 99 %. These results indicated the advantage of sintering by SPS that attained highest RD for these composites in comparison with those produced for the same compositions by conventional sintering (pressureless) which reached a maximum RD of nearly 65 % at 1400°C as shown in a previous study [20]. In the case of plasma sintering process, there is the direct application of pulsed electric current that rapidly heated the graphite die and can generate a discharge between the particles of the powder (that clean and activate the surfaces). In addition, high heating rates suppress mechanisms of surface diffusion, thereby limiting grain growth, whereas possibly enhance several mass transfer mechanisms such as volume diffusion and grain boundary which lead to a high densification. Also the applied pressure favorably contributed to enhance densification.

Moreover recently was investigated the effects of the high temperature conductivity of zirconia in improving densification process during sintering by SPS. In this study commercial powders of zirconia YZS-8 mol. % Y<sub>2</sub>O<sub>3</sub> with an average particle size of 50 μm were sintered by SPS by applying pressure of 40 MPa and a heating rate of 80°C min<sup>-1</sup>, for 20 minutes between 800 - 1200°C [26]. The authors showed that sintering at high temperatures (800°C or more) increases the conductivity of the zirconia and for this reason the powder can be subject to a direct electric heating (through the powder). Other previous studies reported that this effect contributes to the neck formation process during SPS [27-31].

Moreover for ZC and ZCF composites RD increased with increasing sintering temperature. This effect of thermal treatment on RD was more significant in ZC composites.

For ZCF composites the low particle size of the zirconia as starting powder enhanced the driving force and the kinetics of the sintering process. This effect lead to a higher degree of densification in ZCF composites and thus the effect of sintering temperature on increasing RD was less significant as compared with that of RD of ZC composites. In general the RD of ZCF composites resulted slightly higher than the RD of ZC composites.

At 1400°C the effectiveness of thermal treatment determined the highest RD for ZC and ZCF composites. Except for ZC30 composite containing larger amount of CA<sub>2</sub> for which RD slightly decreased between 1300 and 1400 °C. This may be attributed to microcracking resulting from mismatch in thermal expansion coefficients of the CA<sub>2</sub> and c-ZrO<sub>2</sub> phases with 4.1 and 10 × 10<sup>-6</sup> °C<sup>-1</sup>, respectively [32,33].

The effects of the specific parameters for the sintering by SPS could be observed analyzing the RD of ZC and ZCF composites sintered by SPS at 1200°C and 1300°C. The ZC and ZCF composites containing 5 and 15 mol. % CaO attained similar RD which were slightly lower than those ZC30 and ZCF30 composites

sintered at the same temperatures. This difference may be attributed to the significant effect of the pressure applied (100 MPa) during SPS on the larger agglomerate size for the mixture with more HAC content. High pressure could reduce the size of agglomerates and less porosity between agglomerates of the powder mixture enhanced densification of the composite even at 1200°C. Contrarily, a different behavior was observed at 1400°C in ZC composites. The ZC5 and ZC15 composites showed similar RD but higher than that of ZC30. Thus, the contribution of pressure applied on densification appeared to be more effective for low sintering temperatures.

### Microstructure

The microstructure of the composites were analyzed by SEM-EDX. Dense SEM microstructure of the ZC5 composites sintered at 1200 and 1400°C (Figures

5a, b) consisted of a continuous matrix of ZrO<sub>2</sub> (light gray area) identified by EDX as the principal volume phase with dispersed CA<sub>2</sub> grains (dark gray areas). The CA<sub>2</sub> as isolated grains (sizes ranging between 10 and 50 μm) were distributed throughout the matrix. The CA<sub>2</sub> was the only phase containing alumina present in these composites (Figures 1 and 2). At 1400°C, the dispersed CA<sub>2</sub> grains appeared smaller as a result of more c-ZrO<sub>2</sub> stabilization with temperature (Figure 3).

Figures 5c and d show that grain size of remaining CA<sub>2</sub> reduced notably for ZCF composites. At 1400°C, enhancement of Ca ion diffusion from the CA<sub>2</sub> phase promoted the c-ZrO<sub>2</sub> formation, and finer particles of ZrO<sub>2</sub> favored the reactivity between the ZrO<sub>2</sub> and Ca ion.

Figures 6a and b show that a coarser microstructure resulted with increasing CaO content from 5 to 30 mol. %, due to the increase in the amount of CA<sub>2</sub> relative to ZrO<sub>2</sub>. These microstructures were characterized by interconnected grains of two phases without

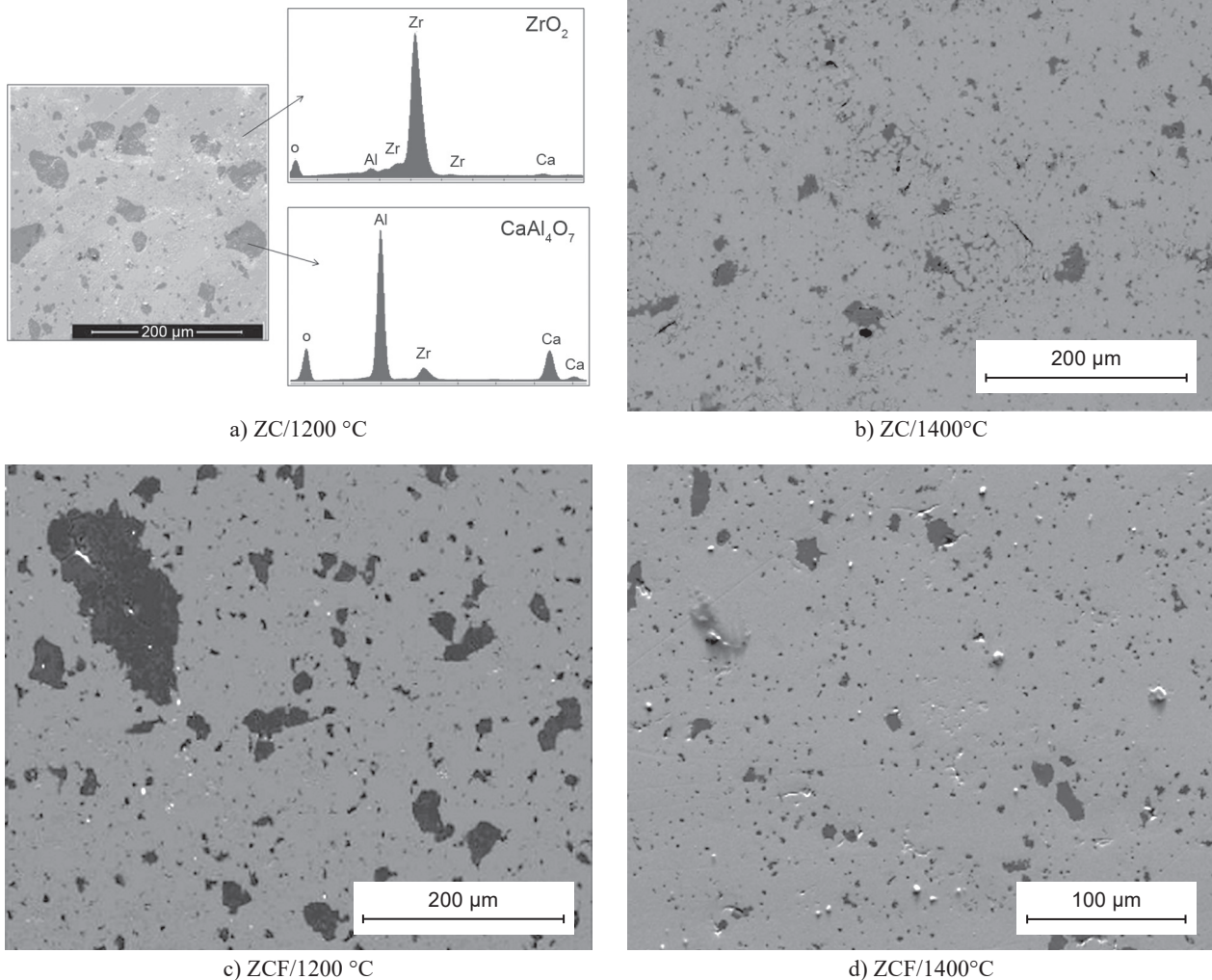


Figure 5. SEM micrographs of composites with 5 mol. % CaO; a) and b) ZC (coarse ZrO<sub>2</sub>) sintered at 1200 and 1400°C, respectively; c) and d): ZCF (fine ZrO<sub>2</sub>) sintered at 1200 and 1400°C, respectively.

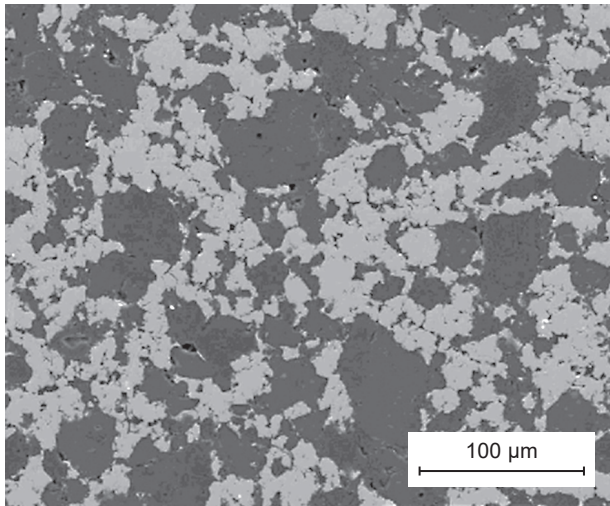
distinguishing a continuous matrix. On the other hand, the microstructure of ZCF30 composites (Figures 7a, b) consisted of a fine zirconia matrix surrounding the dispersed  $CA_2$  grains of variable sizes. The microstructure of these composites was similar even at after sintering at high temperatures .

#### Hardness

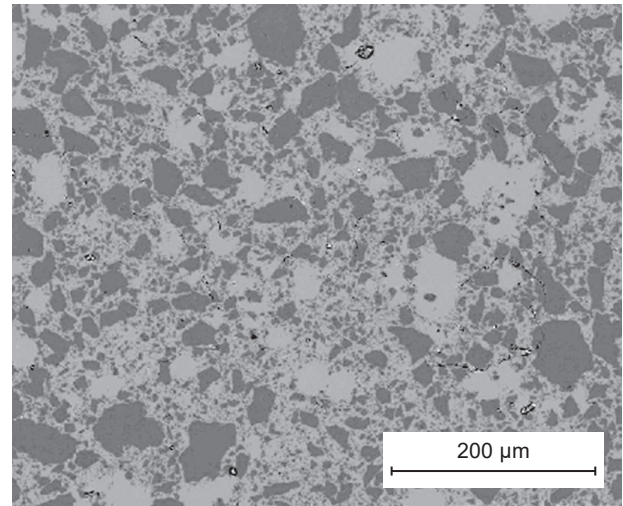
Figures 8a and b show the hardness evolution with temperature for ZC and ZCF composites, respectively.

The hardness of ZC composites sintered between 1200 and 1400°C varied between 7.8 and 9.4 GPa. This result was in agreement with that of previously reported for 8 - 16 mol. % calcia doped zirconia. Such ceramics achieved RD higher than 90 % via microwave sintering at 1585°C 1h and exhibited Vickers hardness of 8 - 9 GPa [17].

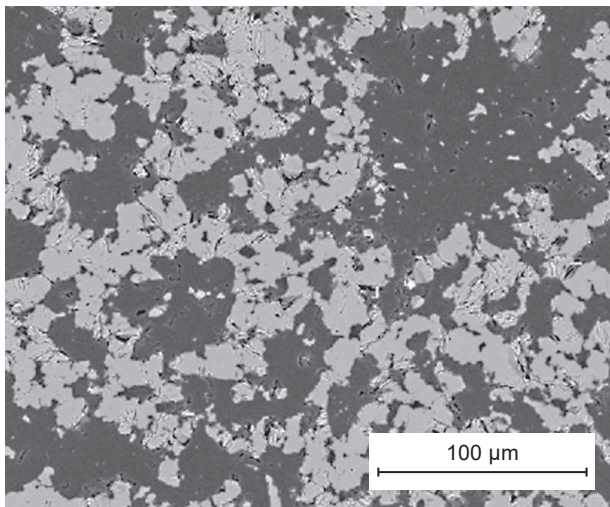
Although a minor difference in hardness between ZC and ZCF composites existed, a different trend can be noted when this property was correlated with the microstructure and porosity. Most of ZC composites presented a moderate hardness near to 9 GPa. In general, the best hardness agreed well with high densification of composites. The lowest hardness about 8 GPa corresponded to the ZC15 composite after SPS at 1200°C and also to the ZC30 composite sintered at 1400°C. In the first case, the decrease in hardness may be associated with the relatively high porosity of the composite (~7%). Contrarily, low hardness of ZC30 composite having a lower porosity was attributed to the significant amount of  $CA_2$  relative to  $c-ZrO_2$  in this composites. There is a difference in hardness (at zero porosity) of each crystalline phases present in the sintered composites being 10, 12, and 11 GPa for  $m-ZrO_2$ ,  $c-ZrO_2$  and  $CA_2$ , respectively [18, 34, 35]. Thus, reduction in hardness with  $CA_2$



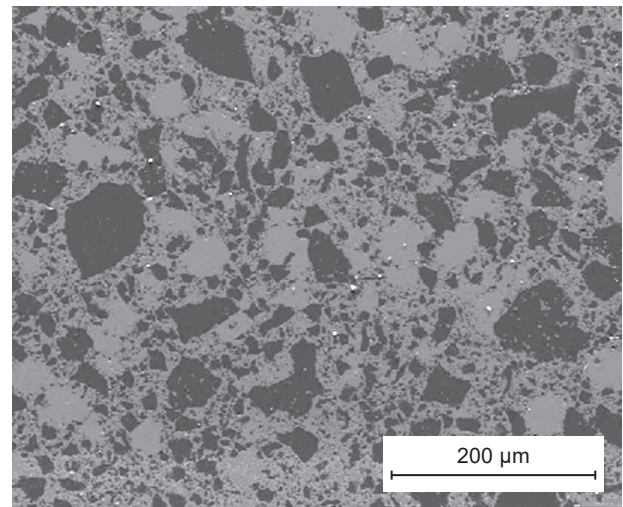
a) 1200°C



a) 1200°C



b) 1400°C



b) 1400°C

Figure 6. SEM micrographs of ZC30 composites (coarse  $ZrO_2$ ) sintered at different temperatures; a) 1200°C; b) 1400°C.

Figure 7. SEM micrographs of ZCF30 composites (fine  $ZrO_2$ ) sintered at different temperatures; a) 1200°C, b) 1400°C.

content may be explained by both the relatively low hardness of this phase and the different microstructure of composites. In comparison, Figures 5 and 7 show that the increase in  $CA_2$  amount changed the microstructure of composites as compared to that of ceramics having low HAC contents. The microstructure of low HAC composites was characterized by the dispersion of few and small  $CA_2$  grains in a dense  $ZrO_2$  matrix. Whereas the microstructure of ZC30 sample containing similar proportion of c- $ZrO_2$  and  $CA_2$  phases was characterized by large interconnecting grains of both phases (i.e. without distinguishing one continuous phase as a matrix). In addition, the presence of some microcracks explained the reduction in hardness of this sample.

Hardness of the ZCF ceramics resulted similar and approximated to 9 - 10 GPa (Figure 8 b). The slightly lower hardness (9 GPa) corresponded to ceramics with 5 and 15 mol. % CaO (i.e. low cement compositions) sintered at 1200 and 1300 °C and to ZCF30 composite sintered at 1300 and 1400°C. In the first case, the lower

hardness was due to porosity above 4 % which was comparatively higher than that of the other composites (2 %). The lower hardness of ZCF30 composites sintered at 1300 and 1400°C did not correlate with porosity but it was probably due to the changes in the microstructure with increasing  $CA_2$  amount. In general, ZCF materials exhibited low porosity and finer grain sizes and consequently reached higher hardness in relation to that of the ZC composites.

## CONCLUSIONS

Dense Calcia stabilized zirconia –  $CA_2$  ( $CaAl_4O_7$ ) composites were produced by SPS from m- $ZrO_2$  and calcium aluminate cement (HAC) mixtures in a range of 1200 - 1400°C. According to the high efficiency of this sintering technique, composites exhibited a high density (93 - 99 % of theoretical density) regardless of the sintering temperature and composition. Moreover, the composites with high CaO content sintered by SPS exhibited high densification even at 1200°C indicating the effectiveness of this technique in comparison with the conventional sintering. Furthermore, the SPS process derived in a strong activation of diffusion processes involved in the reaction of CaO-stabilized zirconia. Both high densification and complete c- $ZrO_2$  formation occurred at a relatively lower temperature than that required by the conventional sintering. For the composites with low CaO content, the c- $ZrO_2$  formation increased with increasing sintering temperature. Also, the reduction of m- $ZrO_2$  particle size promoted the c- $ZrO_2$  formation (even by sintering at low temperatures), but did not have a significant influence on the densification degree of composites.

The maximum Vickers hardness (10 GPa) attained at 1400°C for the composites with low CaO content, probably due to the combined effect of low porosity and SEM microstructure of fine  $ZrO_2$  matrix with small  $CA_2$  grains dispersed. While for composites with high CaO content sintered at the same temperature, the relative lower hardness near of 9 GPa was attributed to the coarser microstructure formed by large interconnecting grains of  $CaAl_4O_7$  and c- $ZrO_2$  phases.

## REFERENCES

1. Munir Z. A., Quach D V., Ohyanagi M.: *J. Am. Ceram. Soc.* 94, 1 (2011).
2. Olevsky E. A., Froyen L.: *J. Am. Ceram. Soc.* 92, 122 (2009).
3. Langer J., Hoffmann M., Guillon O.: *J. Am. Ceram. Soc.* 94, 131 (2011).
4. Munir Z. A., Anselmi-Tamburini U., Ohyanagi M.: *J. Mat. Sci.* 41, 763 (2006).
5. Omori M.: *Mat. Sci. Eng. A* 287, 183 (2000).

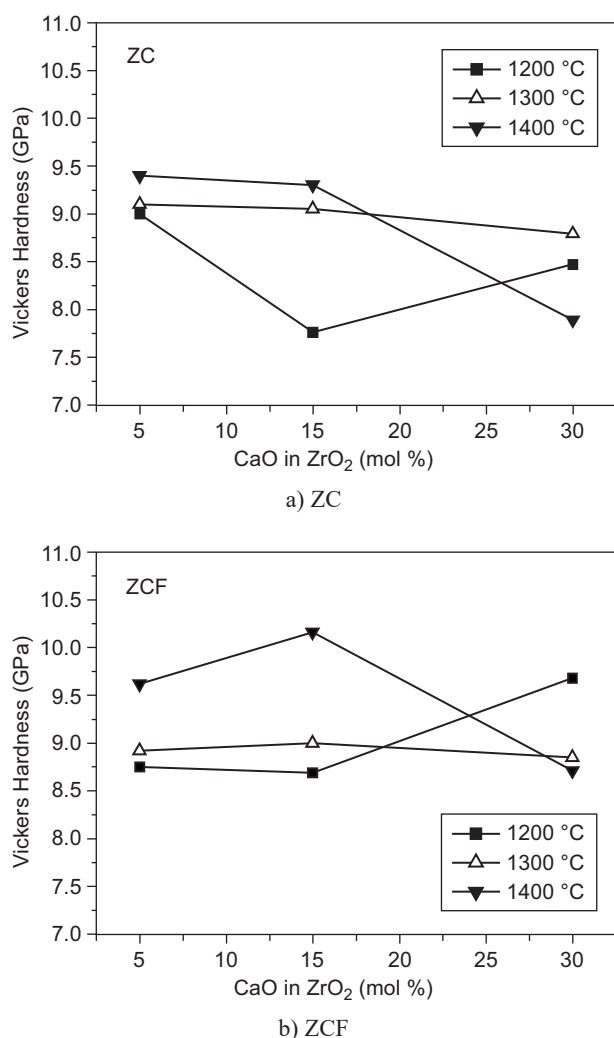


Figure 8. Hardness of composites with 5-30 mol. % CaO sintered at 1200-1400°C; a) ZC composites (coarse  $ZrO_2$ ), b) ZCF composites (fine  $ZrO_2$ ).

6. Orru R., Licheri R., Locci A.M., Cincotti A., Cao G.: *Mat. Sci. Eng. R: Reports* 63, 127 (2009).
7. Nygren M., Shen Z.: *Solid State Sciences* 5, 125 (2003).
8. Schwarz S., Guillon O.: *J. Europ. Ceram. Soc.* 33, 637 (2013).
9. Shen Z., Johnsson M., Zhao Z., Nygren M.: *J. Am. Ceram. Soc.* 85, 1921 (2002).
10. Chakravarty D., Bysakh S., Muraleedharan K., Rao T. N., Sundaresan R.: *J. Am. Ceram. Soc.* 91, 203 (2008).
11. Aman Y., Garnier V., Djurado E.: *J. Am. Ceram. Soc.* 94, 2828 (2011).
12. Demuynck M., Erauw J.-P., Van der Biest O., Delannay F., Cambier F.: *J. Europ. Ceram. Soc.* 32, 1957 (2012).
13. Gurt Santanach J., Weibel A., Estournès C., Yang Q., Laurent Ch., Peigney A.: *Acta Mater.* 59, 1400 (2011).
14. Li W., Gao L.: *J. Europ. Ceram. Soc.* 20, 2441 (2000).
15. Bernard-Granger G., Guizard Ch.: *Acta Mater.* 55, 3493 (2007).
16. Hannink R. H. J.: *J. Am. Ceram. Soc.* 83, 461 (2000).
17. Muccillo R., Buissa Netto R.C., Muccillo E.N.S.: *Mat. Lett.* 49, 197 (2001).
18. Nath S., Sinha N., Basu B.: *Ceram. Intern.* 34, 1509 (2008).
19. Durrani S.K., Akhtar J., Ahmad M., Hussain M.A.: *Mat. Chem. Phys.* 100, 324 (2006).
20. Bruni Y.L., Garrido L.B., Aglietti E.F.: *Ceram. Intern.* 38, 4237 (2012).
21. Dudek M.: *Mat. Res. Bull.* 44, 1879 (2009).
22. Parker K.M., Sharp J.H.: *Trans. J. Br. Ceram. Soc.* 81, 35 (1982).
23. Braulio M.A.L., Morbioli G.G., Milanez D.H., Pandolfelli V.C.: *Ceram. Inter.* 37, 215 (2011).
24. Garvie R., Nicholson P.S.: *J. Am. Ceram. Soc.* 55, 303 (1972).
25. Muromura T., Hinatsu Y.: *Mat. Res. Bull.* 21, 61 (1986).
26. Rajeswari K., Buchi Suresh M., Hareesh U.S., Srinivasa Rao Y., Das D., Johnson R.: *Ceram. Int.* 37, 3557 (2011).
27. Chen X.J., Khor K.A., Chan S.H., Yu L.G.: *Mater. Sci. Eng. A* 341, 43 (2003).
28. Demirsky D., Borodianska H., Grasso S., Sakka Y., Vasylykiv O.: *Scr. Mater.* 65, 683 (2011).
29. Frei J.M., Andelmi-Tamburini U., Munir Z.: *J. Appl. Phys.* 101, 114 (2007).
30. Liu J X., Song X., Zhang J.: *J. Am. Ceram. Soc.* 89, 494 (2006).
31. Quach D.V., Avila-Paredes H., Kim S., Martin M., Munir Z.A.: *Acta Mater.* 58, 5022 (2010).
32. Skinner G.B., Johnston H.L.: *J. Chem. Phys.* 21, 1383 (1953).
33. Suzuki Y., Ohji T.: *Ceram. Int.* 30, 57 (2004).
34. Asmi D., Low I.M.: *J. Mat. Sci. Lett.* 17, 1735 (1998).
35. Gritzner G., Steger P.: *J. Eur. Ceram. Soc.* 12, 461 (1993).